ENVIRONMENTAL RESEARCH
LETTERS

ACCEPTED MANUSCRIPT • OPEN ACCESS

On the anomalous development of the extremely intense positive Arctic Oscillation of the 2019-2020 winter

To cite this article before publication: Ana Juzbaši *et al* 2021 *Environ. Res. Lett.* in press https://doi.org/10.1088/1748-9326/abe434

On the anomalous development of the extremely intense positive Arctic Oscillation of the 2019-2020 winter

A. Juzbašić[1], V.N. Kryjov[1], and J.B. Ahn[1]

[1]Climate Prediction Lab, Department of Earth Environmental System, Pusan National University, Busan, South Korea

Corresponding author: Joong-Bae Ahn (jbahn@pusan.ac.kr)

Abstract

Numerous extreme climate anomalies were recorded in the northern extratropics in January-March (JFM) 2020, significantly impacting human lives and ecosystems in the affected areas. Those anomalies were caused by an extreme positive Arctic Oscillation (AO) event, with the JFM 2020 AO index of 2.8 being the highest on the record. However, all well-established autumn precursors pointed towards the following wintertime AO phase being negative. Indeed, a negative AO phase was developing until late December when a sudden shift to the strong positive AO event occurred in the troposphere. The geopotential anomalies associated with positive AO spread into the lower stratosphere, and were steadily enhancing throughout JFM resulting in an extreme positive AO event. We show that the strong positive AO event was a result of the destructive interference of the anomalous planetary waves with climatological ones, which led to wave flattening and enhancement of the polar vortex.

1 Introduction

The winter of 2019-20 was marked by numerous extreme climate anomalies. New wintertime temperature and precipitation seasonal highs were recorded over northern Eurasia, eastern Asia, and south-eastern North America. It was the first winter when no stable snow cover was recorded in the central East European Plain which resulted in dramatic changes in the regional river discharge annual cycle and the associated human activity. These anomalies impacted human lives not only during the winter, but also in the subsequent seasons. The snow depth and the intensity of snow melt impact the rivers of Barents Sea Basin – positive temperature anomalies in late winter and early spring cause earlier melting of the snow, which leads to the earlier, more intense spring floods in the northern European Russia (Kryjov and Gorelits, 2019), as well as the rivers that feed the Caspian Sea, whose shoreline is incredibly vulnerable to any inflow changes (Akbari et al., 2020). Additionally, in Siberia, the record temperature anomalies and the unstable snow cover which melted early led to the hottest spring on the record, as well as unprecedented wildfires burning forests and peatlands in the spring and summer season of 2020 (Witze 2020), impacting vulnerable areas such as the Eurasian Dryland belt (Groisman et al., 2018). Along with direct, simultaneous negative effects from fire and smoke, these fires also contribute to the faster melting of the permafrost, which is already impacted by climate change (e.g. Vasiliev et al., 2020). Both burning of the peatlands and melting of the permafrost release additional carbon dioxide to the atmosphere which then contributes to the faster warming of the atmosphere (e.g., Groisman and Soja, 2009). At the same time, melting of the permafrost can affect the human lives and the ecosystems alike trough the problems such as erosion and land collapses (Turetsky at al., 2019) and reappearance of the viruses and bacteria that have been trapped in the frozen soil, such as anthrax (Revich and Podolanya, 2011).

The wintertime weather and climate in these areas are strongly affected by the Arctic Oscillation (AO), a dominant mode of the boreal winter extratropical atmospheric variability (Thompson and Wallace, 1998, 2000). The positive wintertime AO phase is associated with a tighter and stronger polar vortex, enhanced zonal and weakened meridional circulation, northward shift of the polar front over Eurasia, warmer and wetter weather over northern Eurasia and south-eastern North America, and colder in the north-eastern North America and Greenland and vice versa during the negative phase (Thompson and Wallace, 1998, 2000). The intensity of spring floods (Kryjov and Gorelits, 2019) and the intensity of southeastern Siberian wildfires have been linked to the preceding wintertime AO (Kim et al 2020). The wintertime AO strongly impacts the concurrent and post-winter environment particularly over Northern Eurasia, the domain of the Northern Eurasia Future Initiative (NEFI) studies (Groisman et al., 2017; Soja and Groisman, 2018).

The AO index features strong interannual and interdecadal variability (e.g., Kryzhov and Gorelits, 2015). The length of the reconstructed and estimated AO index series is about 120 years. However, in terms of the AO index, two extreme wintertime AO events of the opposite polarities occurred within the recent 30 years, in the winters of 1988-89 and 2009-10. The former was a winter of the extremely positive AO event, while the latter was of the extremely negative one. The winter of 2009-10 was detailed by Cohen et al (2010) and Wang and Chen (2010). They have shown that the extreme negative AO event was caused by the anomalous upward propagation of the planetary waves from the troposphere, which excited two sudden stratospheric warmings and the destruction of the polar vortex. The new extreme AO event of positive polarity occurred in the winter of 2019-20. This event was described comprehensively by Lawrence et al.

(2020), who reported, among others, the extremely cold and strong polar vortex in the stratosphere, which led to ozone depletion and extremes in the surface variables associated with the positive AO phase.

Prediction of the wintertime AO polarity and intensity is of crucial importance for adaptation to the wintertime and postwinter anomalous environmental and socio-economic conditions in Northern Eurasia. According to the numerous model and statistical studies on the precursors of the wintertime AO polarity, we could expect the positive phase of the AO to be preceded by a number of specific anomalies in various environments (e.g., Folland et al., 2011; Scaife et al., 2014; Sun and Ahn, 2015; Kumar and Chen, 2018). In particular, several precursors have been identified in the sea surface temperature (SST) anomalies, such as an autumn-developing La Niña (e.g., Bell et al., 2009; Hall et al., 2014, Fletcher and Cassou, 2015) which leads to destructive interference of the generated anomalous long waves (wave numbers 1 and 2) with the climatological ones, a negative SST anomaly in the North Atlantic subpolar gyre (Frankignoul, 1985; Rodwell et al., 1999), and a negative SST and positive sea ice concentration (SIC) anomalies in the Barents and Kara Seas (e.g., Jaiser et al., 2012; Scaife et al., 2014; Kim et al, 2014; Yang et al., 2016; Zhang et al., 2018) which enhance zonal circulation due to increased temperature gradient between the middle and polar latitudes. A number of studies have also shown that the positive phase of the wintertime AO is preceded by a smaller autumn snow cover extent (SCE) and slower snow cover propagation southward in eastern Siberia (Cohen et al., 2007; Cohen and Jones, 2011), as well as a larger anomalous SCE in the middle latitudes of eastern Europe than in eastern Asia (Han and Sun, 2018). Additionally, some autumn circulation patterns were found to precede the positive phase of the wintertime AO. Particularly, the negative middle troposphere geopotential height anomalies over the Taymyr Peninsula (Kryjov and Min, 2016) and the suppressed development of the Ural blocking (Peings et al., 2019). The named snow and circulation anomalies lead to weakening of the East Asia trough due to warmer surface and less cold advection to East Asia in the lower troposphere. With few exceptions, relationships between the wintertime AO index and the listed precursors are linear, so the inverse precursors to those listed above indicate that the wintertime AO phase is expected to be negative. The mechanism of the autumn surface/tropospheric precursors' impact on the wintertime AO implies linear interference between the climatological stationary waves and the forced anomalous waves in the stratosphere, with the peak response, that is, constructive or destructive interference, occurring mainly in January (Smith et al., 2011; Smith and Kushner, 2012).

All of the listed above autumn 2019 precursor anomalies indicated that the forthcoming wintertime AO phase should have been negative or at least neutral rather than extremely positive. The observed AO index for the JFM 2020 was, contrary to expectation, the highest on record. That contradiction between the expected and the observed phase of the wintertime AO motivated the present study.

2 Data and methods

The gridded monthly values for the mean sea level pressure (SLP), monthly and daily values for the geopotential height, and the daily values for air temperature were provided on a 2.5° × 2.5° horizontal grid, and the monthly values for the near-surface air temperature (T2m) were provided on the global T62 Gaussian grid, as a part of the National Centers for Environmental Prediction (NCEP)- Department of Energy (DOE) Atmospheric Model Intercomparison Project II's Reanalysis 2 (Kanamitsu et al., 2002) and span from 1979 to the present time.

For the monthly means of sea surface temperature, Extended Reconstructed Sea Surface Temperature (ERSST) v5, derived from International Comprehensive Ocean–Atmosphere Dataset (ICOADS), and available on a global 2°× 2° grid (Huang et al., 2017) was used. Monthly sea ice concentration (SIC) was taken from the Hadley Centre Global Sea Ice and Sea Surface Temperature dataset (HadISST, Rayner et al., 2003). The dataset utilized for the monthly precipitation averages was the Global Precipitation Climatology Project's monthly precipitation dataset (GPCP v.2.3, Adler et al., 2003). Additionally, monthly- and seasonal- mean AO indices (Thompson and Wallace, 1998, 2000) were taken from the NOAA Climate Prediction Center website. Lastly, the monthly mean snow cover extent data were derived from the Rutgers University Global Snow Laboratory data meshed on the irregular 88×88 grid

Climatology was calculated using the values from 1979-2018 for October, November, and December, and from 1980-2019 for January, February, and March. Monthly and seasonal anomalies of the autumn and winter of 2019-2020 were calculated by subtracting the corresponding climatology from the 2019-2020 values. Daily geopotential height anomalies were calculated by subtracting the climatology from the 2019-2020 data, averaging over the polar cap (poleward of 65°N) and normalizing by the standard deviation from the climatological period. The vertical wave activity fluxes (F_Z) were estimated using the methodology developed by Plumb (1985). The 10-day mean anomalies of F_Z at the 100hPa surface and geopotential height of the 70hPa surface from December 1, 2019 – March 29, 2020 were calculated by averaging the daily data over successive 10-day periods and subtracting the corresponding climatology.

The correlation coefficients between several precursors and the January AO index were calculated based on the 40-year detrended series from 1979-2018 for precursors and 1980-2019 for the AO index. All of the indices shown are significant at the 95% confidence level at least (two-tailed test using a Fisher's z-transformation), accounting for the effective sample size (Bretherton et al., 1999). The similarities between the patterns of anomalies were assessed using the spatial congruence coefficients, which are also referred to as an unadjusted anomaly correlation coefficient (Wilks, 2011, Section 8.6.4). All of the shown congruence coefficients are significant at the 95% confidence level at least (one-tailed test based on the Monte-Carlo simulation).

3 Results and discussion

3.1. The JFM 2020 AO index and environmental anomalies

The JFM 1989 AO index was the highest on the record (+2.6) until the winter of 2020 (Fig. 1a), when the new highest positive JFM AO index was documented (+2.8). The JFM SLP anomaly pattern (Fig. 1b) closely resembles that of the AO, with the negative SLP anomaly over the polar area and two centers of the positive anomalies, Atlantic and Pacific. The geopotential height of 500hPa surface (Z500) anomalies show quite a zonally symmetric pattern (Fig. 1c) with almost uninterrupted belt of the positive anomalies in the middle latitudes. However, conversely to the typical AO pattern, the SLP and Z500 anomalies were stronger in the Pacific center than in the Atlantic one in 2020.

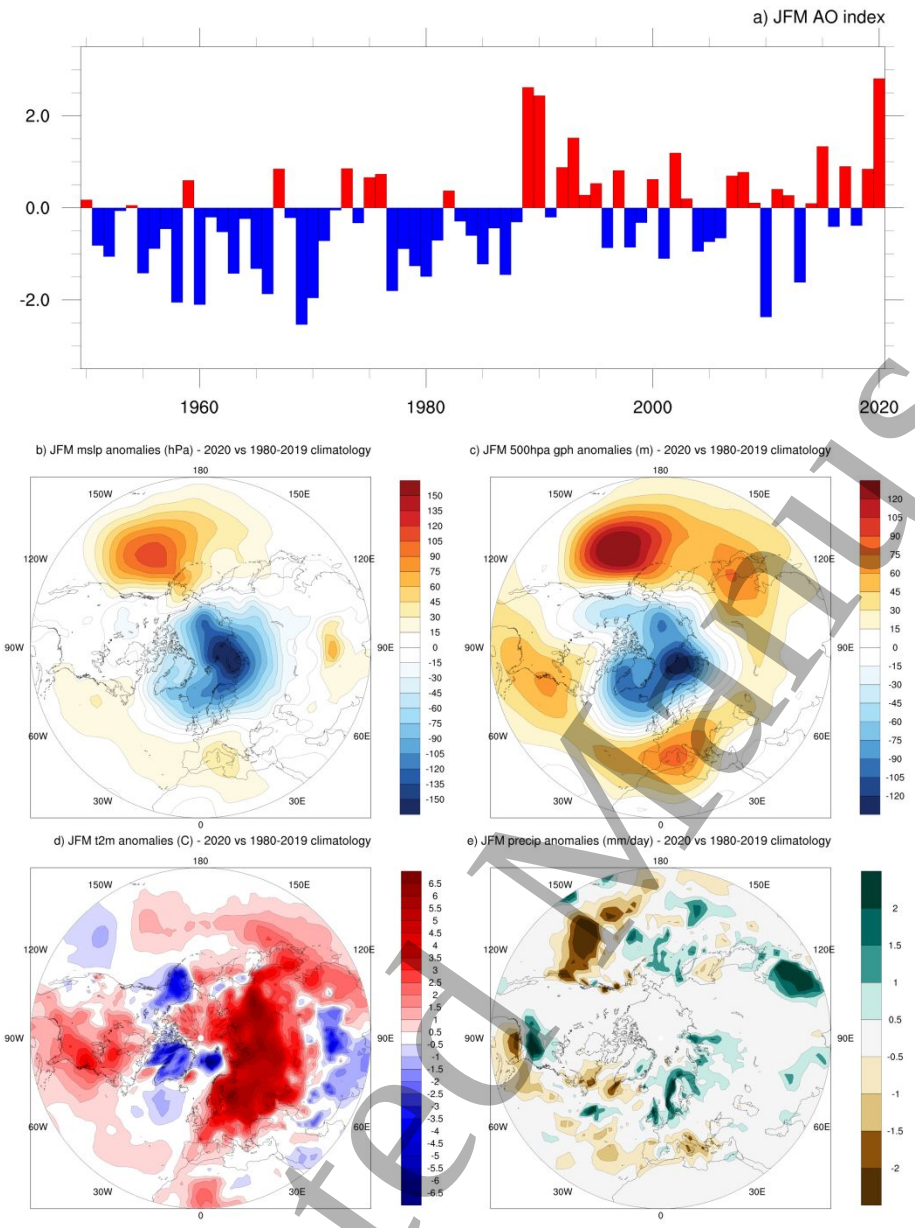

Figure 1. Time series of the JFM AO index (a) and observed JFM 2020 anomalies of (b) mean SLP (hPa), (c) Z500 (m), (d) T2m (°C) and (e) precipitation rate (mm/day).

The T2m anomaly pattern of JFM 2020 shown in Fig. 1d was typical for the positive AO phase (Thomson and Wallace, 2000). Record breaking positive anomalies of up to 7˚C spanned the north-western Eurasia and eastern Asia, with the highest anomalies being recorded in the Siberian region, the NEFI domain. It is worth noting that more than half of the amplitude of these anomalies is congruent with the AO (Lawrence et al., 2020).

The positive anomalies of up to 3.5˚C were observed in south-eastern North America. Meanwhile, north-eastern North America and Greenland featured strong negative T2m anomalies. The only difference from the general AO-related T2m anomaly pattern was the absence of the northern Africa negative anomalies caused by the weakness of the Atlantic SLP/Z500 center. Although the AO is not strongly manifested in precipitation, the precipitation pattern of JFM 2020 (Fig. 1e), particularly the interrupted strip of enhanced precipitation from south-eastern North America via the North Atlantic through the Taymyr Peninsula, definitely shows the shift of the polar front northward over the Atlantic-western Siberian sector (Hall et al., 2014) which is typical for the positive AO phase (Kryzhov and Gorelits, 2015).

Thus, the JFM 2020 SLP and Z500 anomalies as well as the temperature and precipitation anomalies revealed an extremely strong positive phase of the AO, with the JFM AO index being the highest on the record, at least since the early 20th Century.

3.2. The autumn 2019 precursors

Given October and November precursors, we might have expected the wintertime AO index to be negative in 2020. Figure 2 shows the SST anomalies for October and November (ON, hereafter), and the sea ice anomalies for October preceding three extreme AO winters (2019, 2009 and 1988). In ON 2019, the positive SST anomalies (Fig. 2a) covered the equatorial central Pacific, with the Niño3.4 index being positive (+0.5). Similar positive SST anomalies and the positive Niño3.4 index (+1.3) were observed in ON 2009 (Fig. 2b) preceding the extremely negative AO winter. On the other hand, in 1988, before the extremely positive AO winter, the SST anomalies in the equatorial central Pacific and the Niño3.4 index (-1.8) were negative (Fig. 2c). Thus, the autumn equatorial central Pacific SST anomaly and the ENSO predicted a negative AO phase rather than a positive, in accordance with Bell et al.(2009), Hall et al. (2014), and Fletcher and Cassou (2015). The relationship between the AO indices and the ENSO is not strong (L'Heureux and Thompson, 2005), at least for moderate AO events. However, it is the first occurrence in recorded history where an extreme positive AO event was preceded by a developing El-Niño.

Another precursor is the SST anomaly in the North Atlantic subpolar gyre (Frankignoul, 1985; Rodwell et al., 1999). This was quite positive in 2019, similar to the ON 2009 preceding the extremely negative AO event, with a congruence coefficient between the SST anomaly patterns in the Atlantic belt 50N-80N east of 50W being +0.55. The congruence coefficient with the ON 1988 SST anomalies was -0.51.

The most studied and supported precursor of the wintertime AO polarity is the autumn Barents and Kara Sea (BKS) SIC anomalies, with the relationships being significant for both interannual and trend-like SIC impact on the AO and Northern Eurasia climate (e.g., Petoukhov and Semenov, 2010; Jaiser et al., 2012; Scaife et al., 2014; Kim et al., 2014; Yang et al., 2016; Zhang et al., 2018). The BKS October SIC anomalies (Fig. 2d) were negative, similarly to those of 2009 (Fig. 2e, congruence coefficient +0.8) preceding the extremely negative AO polarity, and opposite to the BKS October positive SIC anomalies of 1988 (Fig. 2f, congruence coefficient -0.66). The correlation coefficient between the October SIC anomalies area-averaged over BKS (60N-85N, 30E-100E) and January AO index is 0.51 on the detrended series and 0.44 on the original ones. The normalized (in respect to 1979-2018 period) October 2019 SIC value was 1.21. Thus, the autumn BKS SIC anomalies also predicted the negative AO phase.

Other precursors, not shown here, also indicated the negative AO polarity for the winter of 2020. According to Smith et al. (2011) and Smith and Kushner (2012), the peak response to the autumn precursors occurs in January. The 2020 January AO index was +2.42. We have "predicted" it with a number of the well-established autumn precursors by linear regression. Over the training period (1980-2019), the AO index mean and standard deviation were -0.08 and 1.39, correspondingly.

Kryjov (2015) documented the strong relationships between the October Taymyr Circulation Index (TCI) and the DJF AO index. The correlation coefficient between October TCI and January AO index was -0.51. Normalized 2019 October TCI was 0.67, predicting January AO index at -0.56. Peings (2019) showed that the positive November Z500 anomaly over the Urals (referred to as the Ural Blocking Index, UBI) tends to precede the negative wintertime AO polarity. The correlation between the November UBI and January AO was -0.43, with the normalized UBI value being 1.17, yielding a January AO index of -0.78. Thus, these two indices indicated that the AO polarity in January tended to be negative. Meanwhile, the QBO signal was very weak, and, in general, the autumn status of the stratosphere did not suggest evolution toward the exclusively positive AO phase (Kryjov and Park, 2007; Peings et al., 2017).

The snow-cover extent anomalies over the eastern Siberian-Mongolian region were positive (figures are available at https://climate.rutgers.edu/snowcover/index.php) in October and November, while the November snow cover extent in north-eastern Europe was below normal, with both the October (Cohen et al., 2007; Cohen and Jones, 2011) and November (Han and Sun, 2018) snow patterns indicating a negative wintertime AO polarity. In particular, the November snow index of Han and Sun (2018), which is defined as the normalized difference between the snow cover anomalies over the Mongolian region and over eastern Europe, which correlates with the January AO index with a coefficient of -0.53, was 1.2, and the linear regression yielded a January AO index of -0.96.

Thus, the state of well-established autumn precursors of the wintertime AO phase, supported by both empirical and model studies and by the use in operational practice, definitely indicated that the JFM 2020 AO phase would be negative or neutral, at least. No autumn precursors indicated the extremely positive AO phase for the forthcoming winter.

Nevertheless, six seasonal prediction systems contributing to the seasonal forecast database of the Copernicus Climate Change Service predicted the correct AO polarity but essentially underestimated its intensity (Lee et al., 2020). The authors also noted that model experiments would be required to allocate the source of predictability fully. Hardiman et al. (2020) suggested that the strong positive Indian Ocean Dipole (IOD) event in autumn 2019 was the source of predictability. However, this specific IOD teleconnection is active when the ENSO is neutral, so it is not a universal predictor. Particularly, the IOD was negative in 1988, preceding the previous extremely positive AO, and positive in 2009 preceding the extremely negative AO. It should also be noted that the prediction of the extratropical Z500 tercile probabilities for JFM 2020 issued by the World Meteorological Organization Lead Center for the Long-Range Forecast Multi-Model Ensemble (WMO LC-LRFMME) was uncertain. That is, the predicted probabilities of the equiprobable tercile categories did not differ significantly from 33%. This multi-model ensemble comprises seasonal predictions from 12 designated WMO Global Producing Centers, including those discussed by Lee et al. (2020). These forecasts are available at wmolc.org (Kim et al., 2016).

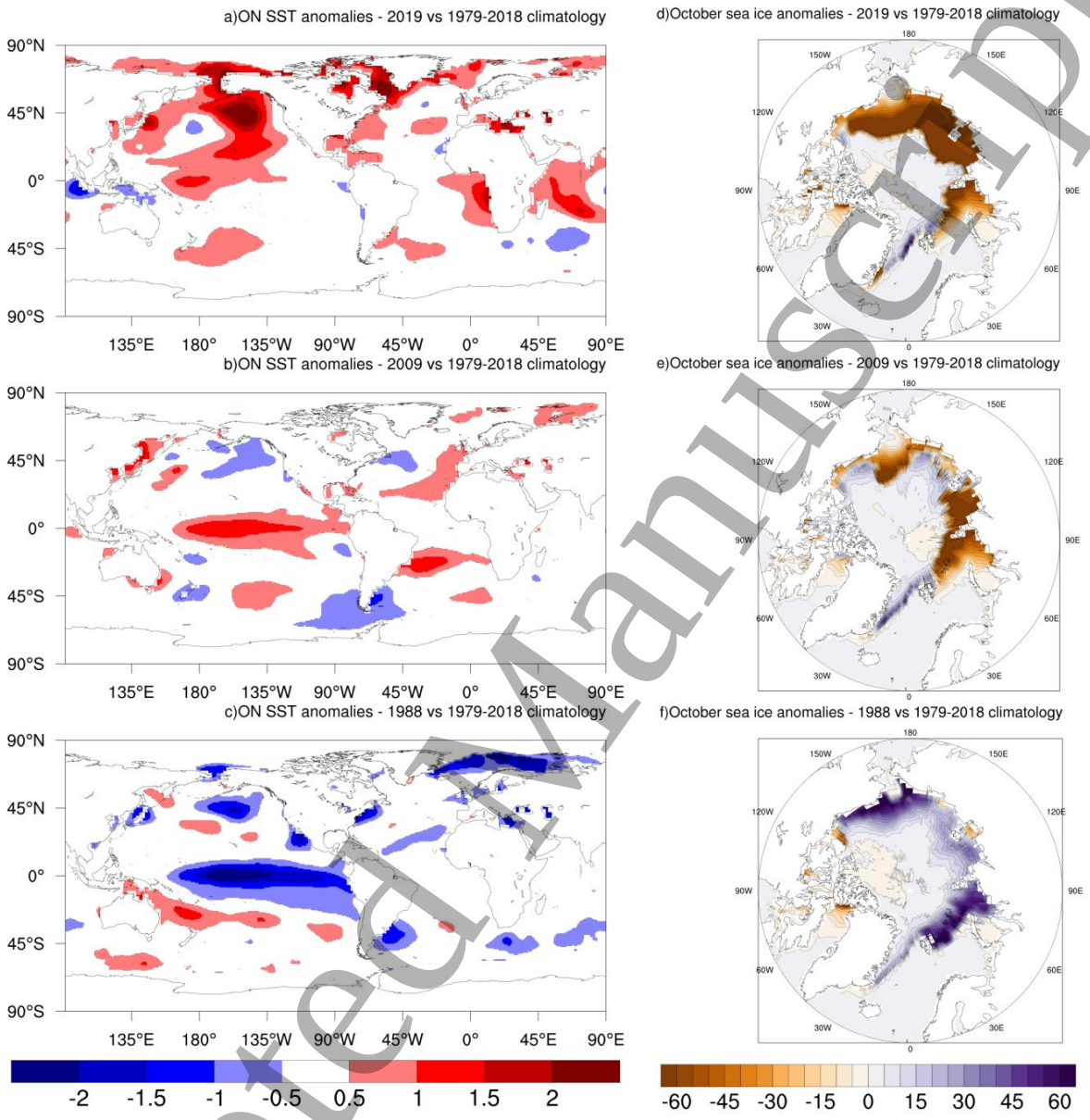

Figure 2. ON anomalies of global SST (°C, a-c) and October anomalies of SIC (%, d-f) for the autumns preceding the winters of the extreme JFM AO index: (a, d) 2020 (positive); (b, e) 2010 (negative); and (c, f) 1989 (positive).

3.3. Evolution of Circulation in October-March 2019-2020

Figure 3 shows the polar cap daily normalized geopotential height anomalies from October 1 to March 31. The positive anomalies spanned the whole troposphere and lower stratosphere in October similarly to 2009 (Fig. 1a of Cohen et al., 2010). In November and December, the development of the negative AO event continued, with the positive anomalies becoming stronger and progressing upwards in November and then back downwards during December. This

evolution closely matches the general scheme of the development of the negative AO event suggested by Baldwin and Dunkerton (2001) and Cohen et al. (2007). Also, this evolution was similar (with some two-three week lag) to that of 2009 (Fig. 1a of Cohen et al., 2010). Therefore, establishing of the moderate positive (at least, near zero) polar cap anomalies in the troposphere was expected. Furthermore, the geopotential height anomalies in the stratosphere were near zero and no negative anomalies could descend in late December.

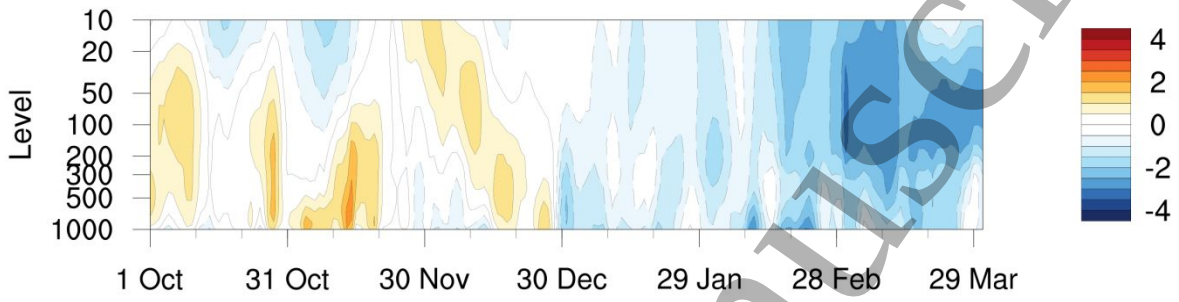

Figure 3. Evolution of the daily normalized anomalies of geopotential height area averaged over the polar cap (65°N-90°N) for the period from October 1st 2019 to March 31st 2020.

However, in contrast to December 2009 when the descending positive anomalies explosively enhanced in the lower troposphere, in late December 2019, the negative geopotential height anomalies suddenly arose in the lower troposphere and spread throughout the whole troposphere and lower stratosphere resembling a scheme of the positive AO event development of Baldwin and Dunkerton (2001). These anomalies persisted all throughout the rest of the winter, steadily enhancing and leading to the most extreme positive JFM AO event in recorded history. Figures 4 and 5 show respectively the 10-day-average F_Z anomalies at 100hPa and geopotential height anomalies of the 70hPa surface over the northern hemisphere (20°N-85°N). The black contours represent respective 10-day climatologies. The vertical wave activity flux, F_Z, is proportional to the meridional eddy heat flux (Plumb, 1985). The anomalous wave activity flux forms anomalous ridges (positive F_Z) or troughs (negative F_Z) above it in the stratosphere, which can lead to the destruction or enhancement of the polar vortex through the interference with the climatological ridges and troughs (Smith and Kushner, 2012).

In the first two decades of December, the directions of the anomalous F_Z mainly coincided with the directions of climatological fluxes (Figs. 4a and 4b), particularly, climatological upward fluxes over eastern Siberia and downward fluxes over northern North America were enhanced by the anomalies. These anomalies were favorable for meandering of the polar vortex and associated negative AO polarity. That was also reflected in the enhancement of the climatological ridge over the eastern North Pacific and troughs over eastern Asia and eastern North America (Figs. 5a and 5b). In the last 10 days of December there were positive F_Z anomalies over north-eastern Asia, enhancing upward climatological flux. However, at the same time, strong downward F_Z anomalies developed over the mid-latitude North Atlantic offsetting the climatological upward flux (Fig. 4c). The corresponding geopotential height anomalies (Fig.5c) were weak but definitely out-of-phase with climatology.

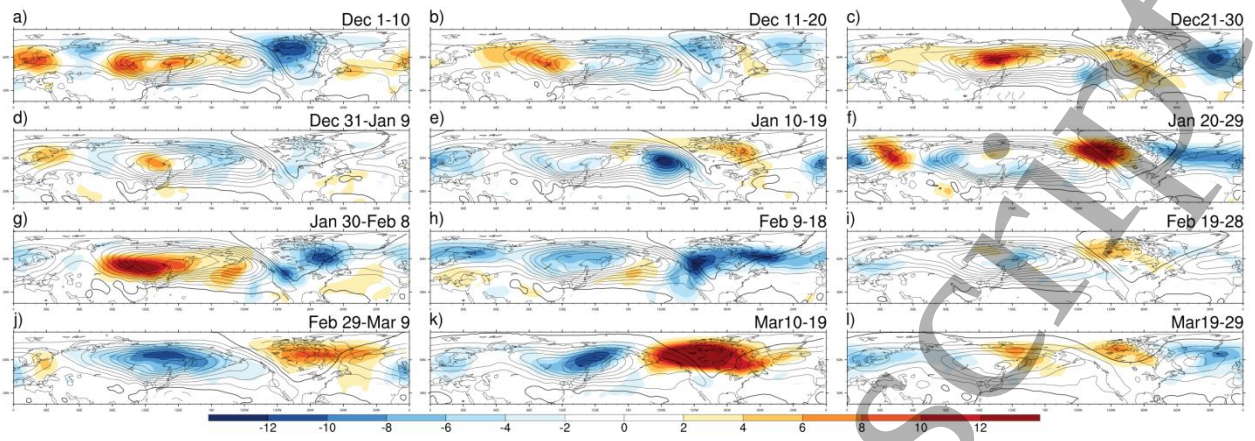

Figure 4. Succession of the 10-day averaged F_Z anomalies (shading, [10^{-3} m^2/s^2]) and climatology (contours) at the 100-hPa surface for 120 days from December 1st until March 29th. Contour interval is 10^{-3} m^2/s^2, negative values are dashed; 0 value contour is of double thickness. Positive climatological values indicate upward flux, while negative values indicate downward flux. The 10-day intervals are shown in the top right hand corner of each panel.

At the beginning of January, the F_Z anomalies were weak (Fig. 4d). However, the enhanced anomalous downward wave activity fluxes occurred over the regions of climatological upward fluxes starting from mid-January (Fig. 4e) and continuing through late March (Fig 4l), with the exception of late January and early February (Fig. 4g). Meanwhile, over northern North America and the American sector of the Arctic, the upward F_Z anomalies prevailed, which were also out-of-phase with climatology. Those anomalies played a role in destructive interference and flattening of the planetary waves and strengthening of the polar vortex. Starting from the first decade of January, the geopotential height was steadily increasing in the middle latitudes and decreasing in the polar area (Fig. 5d – 5l) which were maintaining and enhancing the polar vortex and developed into the extreme positive AO event.

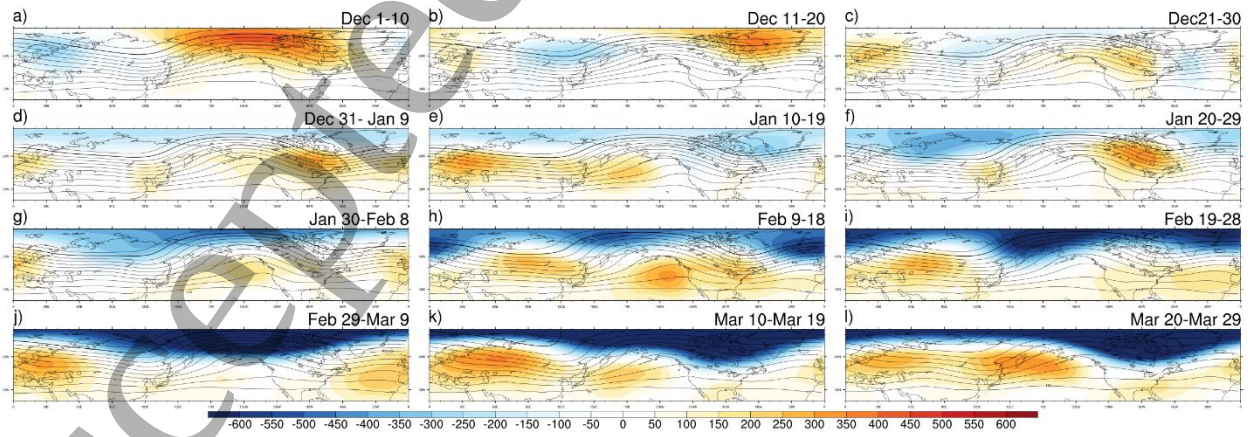

Figure 5. Succession of the 10-day averaged geopotential height anomalies (shading, [m]) and climatology (contours) of the 70-hPa surface for 120 days from December 1st until March 29th. Contour interval is 100m, and the 17,600m value contour is of double thickness. The 10-day intervals are shown in the top right hand corner of each panel.

Thus, in October through December, the moderate negative AO event was developing. Then, in late December, a sudden shift to the development of the positive AO event occurred. Furthermore, from early January through March, there was a definite steady enhancement of the polar vortex, reflected in the intensification of the positive AO event, caused by the F_Z anomalies out-of-phase with climatology and corresponding destructive interference of anomalous and climatological waves. Some weakening of the process in early February did not reverse it. We hypothesize that the shift to the positive AO event in late December was excited by the strong anomalous downward F_Z over the mid-latitude North Atlantic. This anomalous Fz in the lower stratosphere is associated with enhancement of the polar vortex (Jadin, 2011), that is, enhancement of the positive AO event. Furthermore, since the climatological F_Z is upward over the mid-latitude North Atlantic, the strong downward F_Z leads to the destructive interference of the associated planetary waves. Hardiman et al. (2020) showed that the very strong positive autumn IOD event, the second strongest after that of 1997, could have triggered the Rossby wave train originating from the Indian Ocean over the Pacific and towards the North Atlantic, which would be consistent with the anomalies of F_Z observed in late January and early February.

4. Conclusions

The JFM 2020 AO index was +2.8, the highest on the record since the beginning of the 20th Century at least, with the climate anomalies, associated with the positive AO event, being observed. Over large areas, the AO-related anomalies achieved extreme amplitudes, particularly the positive temperature anomalies over northern Eurasia. These have caused undesirable consequences for humans and ecosystems alike, from changes of water cycles to the unprecedented Siberian wildfires, which impacted the already vulnerable areas such as the North Eurasian Dryland belt, the Arctic peatlands, and the Caspian Sea catchment.

The extremely strong and long-lasting polar vortex in 2020 also had the highest potential for chemical destruction of the ozone layer on record, with the FMA column ozone being the lowest since at least 1979 (Lawrence et al., 2020).Meanwhile, the preceding autumn precursors of the wintertime AO phase were favorable for development of the negative rather than positive AO event. And the climate system evolved that way until late December, with the polar cap positive geopotential anomalies steadily descending from the stratosphere to troposphere. However, the negative anomalies suddenly arose in the lower troposphere and then spread throughout the whole atmosphere up to 10 hPa at least. The polar cap negative geopotential anomalies were maintaining and steadily enhancing from January through March. During these three months, the destructive interference of the planetary waves leading to flattening of the waves was distinctly monitored in the lower stratosphere. Associated enhancement of the zonal circulation and weakening of meridional one positively feedbacked on the thermal/geopotential gradient between the middle and high latitudes.

In late December-early January, when the polar cap geopotential anomalies suddenly became negative, strong anomalous downward F_Z occurred over the mid-latitude North Atlantic. The F_Z anomalies were out-of-phase with climatological patterns. Therefore, we suggest that this out-of-phase event may have resulted in the destructive interference of the planetary waves, leading to flattening of the climatological waves and the development of the extreme positive AO event. This is in agreement with Lawrence et al.(2020) in that the stratosphere-troposphere interactions played an important role in the development and persistence of the strong polar vortex and positive tropospheric AO.

However, further investigations should be performed on the triggering mechanism to determine which climate system anomalies triggered the F_Z and geopotential height anomalies which were out of phase with climatological patterns.

The abnormality of the winter of 2020, as well as the consequences of the extreme Artic Oscillation event for both the ecosystem and human lives, have put additional emphasis on the need for improving of both statistical and numerical predictions of the AO polarity and intensity. The winter of 2019-2020 shows the failure of the well-established precursors skillful in the past. The current research was limited to the analysis of the well known precursors and the development of the Arctic Oscillation in the winter of 2019-2020, but further research should be performed to answer the additional questions that emerged during the study, such as what triggered the anomalous F_Z, which other precursors have predicted this winter correctly, what were the sources of predictability in the models and how reliable are the existing precursors in the changing climate.

Acknowledgments

This work was funded by the Korea Meteorological Administration Research and Development Program under Grant KMI2020-01411.

NCEP_Reanalysis 2 (Kanamitsu et al., 2002) data, NOAA_ERSST_V5 (Huang et al., 2017) data, GPCP (Adler et al., 2003.) data, and the monthly Quasi-Biennial Oscillation (QBO) indices are provided by the NOAA/OAR/ESRL PSL, Boulder, Colorado, USA, from their Web site at https://psl.noaa.gov/. HadISST (Rayner et.al., 2003) data were obtained from https://www.metoffice.gov.uk/hadobs/hadisst/ and are © British Crown Copyright, Met Office [2020], provided under a Non-Commercial Government Licence http://www.nationalarchives.gov.uk/doc/non-commercial-government-licence/version/2. Monthly and seasonal AO indices and historical Niño3.4 indices were taken from the NOAA Climate Prediction Center website (http://www.cpc.ncep.noaa.gov/). Snow cover data were provided by Rutgers University (https://climate.rutgers.edu/snowcover/index.php)

References

Akbari M., Baubekova, A., Roozbahani, A., Gafurov, A., Shiklomanov, A., Rasouli, K., Ivkina, N., et.al. (2020) Vulnerability of the Caspian Sea shoreline to changes in hydrology and climate. *Environmental Research Letters 15*, 115002. https://doi.org/10.1088/1748-9326/abaad8

Adler, R. F., Huffman, G. J., Chang, A., Ferraro, R., Xie, P., Janowiak, J., et.al. (2003). The version 2 Global Precipitation Climatology Project (GPCP) monthly precipitation analysis (1979-present). *Journal of Hydrometeorology, 4(6)*, 1147-1167. https://doi.org/10.3390/atmos9040138

Baldwin, M. P., & Dunkerton, T. J. (2001). Stratospheric harbingers of anomalous weather regimes, *Science, 294,* 581–584. https://doi.org/10.1126/science.1063315

Bell, C. J., Gray, L. J., Charlton-Perez, A. J., Joshi, M., & Scaife, A. A. (2009). Stratospheric communication of El Niño teleconnections to European Winter, *Journal of Climate, 22*, 4083–4096. https://doi.org/10.1175/2009JCLI2717.1

Bretherton C, Widmann M, Dymnikov V, Wallace J, Blade I. (1999). The effective number of spatial degrees of freedom of a time-varying field. *Journal of Climate.* **12**: 1990–2009. https://doi.org/10.1175/1520-0442(1999)012<1990:TENOSD>2.0.CO;2

Cohen, J., Barlow, M., Kushner, P. & Saito, K. (2007). Stratosphere-troposphere coupling and links with Eurasian land surface variability *Journal of Climate, 20*, 5335–5343. https://doi.org/10.1175/2007JCLI1725.1

Cohen, J., Foster, J., Barlow, M., Saito, K. & Jones, J. (2010). Winter 2009–2010: a case study of an extreme Arctic Oscillation event. *Geophysical Research Letters, 37*, L17707. https://doi.org/10.1029/2010GL044256

Cohen, J., & Jones, J. (2011**).** A new index for more accurate winter predictions. *Geophysical Research Letters, 38*, L21701. https://doi.org/10.1029/2011GL049626

Fletcher, C. G., & Cassou, C. (2015). The dynamical inuence of separate teleconnections from the paci_c and indian oceans on the northern annular mode. *Journal of Climate, 28* (20), 7985-8002. https://doi.org/10.1175/JCLI-D-14-00839.1

Folland, C.K., Scaife, A.A., Lindesay, J., & Stephenson, D.B. (2011). How potentially predictable is northern European winter climate a season ahead? *International Journal of Climatology, 32*, 801–818. https://doi.org/10.1002/joc.2314

Frankignoul, C. (1985). Sea surface temperature anomalies, planetary waves and air-sea feed-back in the middle latitudes. *Reviews of Geophysics,* 23, 357–390. https://doi.org/10.1029/RG023i004p00357

Groisman, P.Y. & Soja, A.J.(2009). Ongoing climatic change in Northern Eurasia: justification for expedient research. *Environ. Res. Lett*. 4, 045002. https://doi.org/10.1088/1748-9326/4/4/045002

Groisman, P. Y., Shugart, H., Kicklighter, D. Henebry, G., Tchebakova, N., Maksyutov, S., Monier,E., et al.(2017). Northern Eurasia Future Initiative (NEFI): facing the challenges and pathways of global change in the twenty-first century Progress in Earth and Planet Sci 4 41. https://doi.org/10.1186/s40645-017-0154-5

Groisman, P., Bulygina, O., Henerby, G., Speranskaya, N., Shiklomanov, Y.C., Tchebakova, N., Parfenova, E., et.al. (2018). Dryland belt of Northern Eurasia: contemporary environmental changes and their consequences. *Environmental Research Letters 13,* 115008. https://doi.org/10.1088/1748-9326/aae43c

Hall R., Erdélyi R., Hanna E., Jones J.M., & Scaife A.A. (2014). Drivers of North Atlantic polar front jet stream variability. *International Journal of Climatology, 35*, 1697–1720. https://doi.org/10.1002/joc.4121

Han, S., & Sun, J. (2018). Impacts of Autumnal Eurasian Snow Cover on Predominant Modes .628 of Boreal Winter Surface Air Temperature Over Eurasia. *Journal of Geophysical* 629 *Research: Atmospheres*, *123*(18), 10-076. https://doi.org/10.1029/2018JD028443

Hardiman,S.C, Dunstone, N.J., Scaife, A.A., Smith,D.M., Knight, J.R., Davies,P., Claus, M., Greatbatch, R.J. (2020.) Predictability of European winter 2019/20: Indian Ocean dipole impacts on the NAO. *Atmospheric Science Letters 21:e1005*. https://doi.org/10.1002/asl.1005

Huang, B., Thorne P.W., Banzon, V.F., Boyer, T., Chepurin, G., Lawrimore, J.H., et. al., (2017). Extended Reconstructed Sea Surface Temperature version 5 (ERSSTv5), Upgrades, validations, and intercomparisons. *Journal of Climate,30,* 8179-8205. https://doi.org/10.1175/JCLI-D-16-0836.1

Jadin, E.A. (2011). Stratospheric "wave hole" and interannual variations of the stratospheric circulation in late winter. *Natural Science, 3(4),* 259-267. https://doi.org/10.4236/ns.2011.34033

Jaiser, R., Dethloff, K., Handorf, D., Rinke, A. & Cohen, J. (2012). Impact of sea ice cover changes on the Northern Hemisphere atmospheric winter circulation. *Tellus A: Dynamic Meteorology and Oceanography, 64:1*, 11595. https://doi.org/10.3402/tellusa.v64i0.11595

Kanamitsu, M., Ebisuzaki, W., Woollen, J., Yang, S., Hnilo, J. J., Fiorino, M., & Potter G. L., (2002). NCEP–DOE AMIP-II Reanalysis (R-2). *Bulletin of the American Meteorological Society*, *83*, 1631–1644. https://doi.org/10.1175/BAMS-83-11-1631.

Kim, B.-M., Son S.-W., Min S.-K., Jeong J.-H., Kim S.-J., Zhang X.,Shim T., & Yoon J.-H. (2014). Weakening of the stratospheric polar vortex by Arctic sea-ice loss. *Nature 5*, 4646, https://doi.org/10.1038/ncomms5646

Kim, G., Ahn, J.-B., Kryjov, V.N., Sohn, S.-J., Yun, W.-T., Graham, R., Kolli, R.K., Kumar, A., Ceron, J.-P. (2016). Global and regional skill of the seasonal predictions by WMO Lead Centre for Long-Range Forecast Multi-Model Ensemble. *International Journal of Climatology 36,* 1657–167. https://doi.org/10.1002/joc.4449

Kim, J.S., Kug, J.S., Jeong, S.J., Park H., & Schaepman-Strub, G.(2020) Extensive fires in southeastern Siberian permafrost linked to preceding Arctic Oscillation. *Science Advances 6(2),* eaax3308. https://doi.org/10.1126/sciadv.aax3308

Kryjov V.N. (2015). October circulation precursors of the wintertime Arctic Oscillation. *International Journal of Climatology*. **35**: 161–171. https://doi.org/10.1002/joc.3968.

Kryjov V.N. & Gorelits, O.V.(2019) Wintertime Arctic Oscillation and Formation of River Spring Floods in the Barents Sea Basin. *Russian Meteorology and Hydrology 44(3)*, 187–195. https://doi.org/10.3103/S106837391903004X

Kryjov, V.N., & Min, Y.M. (2016). Predictability of the wintertime Arctic Oscillation based on autumn circulation. *International Journal of Climatology*. 36: 4181–4186. https://doi.org/10.1002/joc.4616

Kryjov V.N., & Park C.K. (2007). Solar modulation of the El-Niño/Southern Oscillation impact on the Northern Hemisphere annular mode. *Geophysical Research Letters 34*, L10701. https://doi.org/10.1029/2006GL028015

Kryzhov, V.N., & Gorelits, O.V. (2015). The Arctic Oscillation and Its Impact on Temperature and Precipitation in Northern Eurasia in the 20th Century. *Russian Meteorology and Hydrology 40(11)*:711-721. https://doi.org/10.3103/S1068373915110011

Kumar, A., & Chen, M. (2018). Causes of skill in seasonal predictions of the Arctic Oscillation. *Climate Dynamics, 51*, 2397–2411. https://doi.org/10.1007/s00382-017-4019-9

Lawrence, Z. D., Perlwitz, J., Butler, A. H., Manney, G. L., Newman, P. A., Lee, S. H., & Nash, E. R. (2020). The remarkably strong Arctic stratospheric polar vortex of winter 2020: Links to record-breaking Arctic Oscillation and ozone loss. *Journal of Geophysical Research: Atmospheres, 125,* e2020JD033271. https://doi.org/10.1029/2020JD033271

Lee, S. H., Lawrence, Z. D., Butler, A.H., & Karpechko, A. Y. (2020). Seasonal forecasts of the exceptional Northern Hemisphere winter of 2020. *Geophysical Research Letters, 47,e2020GL090328*. https://doi.org/10.1029/2020GL090328

L'Heureux, M. L., & Thompson D. W. J. (2005). Observed relationships between the El-Niño/Southern Oscillation and the extratropical zonal mean circulation, *Journal of Climate 19,* 276– 287. https://doi.org/10.1175/JCLI3617.1

Peings, Y. (2019). Ural Blocking as a driver of early winter stratospheric warmings. *Geophysical Research Letters. 46 (10)*, 5460-5468. https://doi.org/10.1029/2019GL082097

Peings, Y., Douville, H., Colin, J., Martin, D. S., & Magnusdottir, G. (2017). Snow–(N) AO teleconnection and its modulation by the Quasi-Biennial Oscillation. *Journal of Climate*, *30(24),* 10211-10235 https://doi.org/10.1175/JCLI-D-17-0041.1

Petoukhov, V., & Semenov V. A. (2010). A link between reduced Barents–Kara Sea ice and cold winter extremes over northern continents. *Journal of Geophysical Research, 115*, D21111, https://doi.org/10.1029/2009JD013568 .

Plumb, R. A. (1985). On the Three-Dimensional Propagation of Stationary Waves. J. *Atmos. Sci*., *42,* 217–229. https://doi.org/10.1175/1520-0469(1985)042<0217:OTTDPO>2.0.CO;2

Rayner, N.A., Parker, D.E., Horton E.B., Folland, C.K., Alexander, L.V., Rowell, D.P., et.al. (2003). Global analyses of sea surface temperature, sea ice, and night marine air temperature since the late nineteenth century. *Journal of Geophysical Research, 108(D14),* 4407. https://doi.org/10.1029/2002JD002670

Revich, B.A. & Podolnaya, M.A. (2011) Thawing of permafrost may disturb historic cattle burial grounds in East Siberia, *Global Health Action, 4:1*, https://doi.org/10.3402/gha.v4i0.8482

Rodwell, M. J., Rowell, D. P. & Folland, C. K. (1999). Oceanic forcing of the wintertime North Atlantic Oscillation and European climate, *Nature, 398,* 320–333. https://doi.org/10.1038/18648

Scaife, A.A., Arribas, A., Blockley, E., Brookshaw, A., Clark, R.T., Dunstone, N. et al. (2014). Skillful long range prediction of European and North American winters. *Geophysical Research Letters 41:* 2514–2519. https://doi.org/10.1002/2014GL059637

Smith, K. L. & Kushner, P. J. (2012). Linear interference and the initiation of extratropical stratosphere-troposphere interactions, *Journal of Geophysical Research,117,* D13107. https://doi.org/10.1029/2012JD017587

Smith, K. L., Kushner, P. J., & Cohen, J. (2011). The Role of Linear Interference in Northern Annular Mode Variability Associated with Eurasian Snow Cover Extent. *Journal of Climate, 24,* 6185-6202, https://doi.org/10.1175/JCLI-D-11-00055.1

Soja, A. & Groisman, P. Y. (2018). Earth Science and the integral climatic and socio-economic drivers of change across northern Eurasia: The NEESPI legacy and future direction Environ. Res. Lett. 13 040401. https://doi.org/10.1088/1748-9326/aab834

Sun, J., & Ahn, J.B. (2015). Dynamical seasonal predictability of the Arctic oscillation using a CGCM. *International Journal of Climatology. 35,* 1342–1353. https://doi.org/10.1002/joc.4060

Thompson, D.W.J., & Wallace, J.M. (1998). The Arctic oscillation signature in wintertime geopotential height and temperature fields. *Geophysical Research Letters 25,* 1297–1300. https://doi.org/10.1029/98GL00950

Thompson, D.W.J., & Wallace, J.M. (2000). Annular modes in the extratropical circulation. Part I: month to month variability. *Journal of Climate 13,* 1000–1016. https://doi.org/10.1175/1520-0442(2000)013<1000:AMITEC>2.0.CO;2

Turetsky, M.R., Abbot, B.W., Jones, M.C., Anthony, K.W., Olefeldt, D., Schuur, E.A.G., Koven C. et al. (2019). Permafrost collapse is accelerating carbon release. *Nature 569, 32-34.* https://doi.org/10.1038/d41586-019-01313-4

Vasiliev, A.A., Drozdov, D.S., Gravis, A.G., Malkova, G.V., Nyland, K.E., Streletskiy,D.A. (2020). Permafrost degradation in the Western Russian Arctic. *Envirnmental Research Letters 15(4)* 045001. https://doi.org/10.1088/1748-9326/ab6f12

Wang, L., & Chen, W. (2010). Downward Arctic Oscillation signal associated with moderate weak stratospheric polar vortex and the cold December. *Geophysical Research Letters 37,* L09707. https://doi.org/10.1029/2010GL042659.

Wilks, S.D. (2011). Statistical methods in the atmospheric sciences 3rd ed. *International geophysics series; v. 100, Academic Press*, 704p

Witze, A. (2020). The Arctic is burning like never before - and that's bad news for climate change. *Nature 585*, 336-337. https://doi.org/10.1038/d41586-020-02568-y

Yang X-Y. Yuan, X.& Ting, M. Dynamical Link between the Barents–Kara Sea Ice and the Arctic Oscillation (2016). *Journal of Climate 29*, 5103–5122. https://doi.org/10.1175/JCLI-D-15-0669.1

Zhang, P., Wu Y., Simpson I.R., Smith K.L, Zhang X., De B., Callaghan P (2018). A stratospheric pathway linking a colder Siberia to Barents-Kara Sea sea ice loss. *Science Advances* 25, vol.4.
https://doi.org/10.1126/sciadv.aat6025